AD-A064 662   SMITHSONIAN ASTROPHYSICAL OBSERVATORY CAMBRIDGE MASS   F/G 8/5
               INVESTIGATION OF THE LONG-WAVELENGTH GRAVITY FIELD OF THE OCEAN--ETC(U)
               OCT 78   M C ROUFOSSE   F19628-78-C-0003
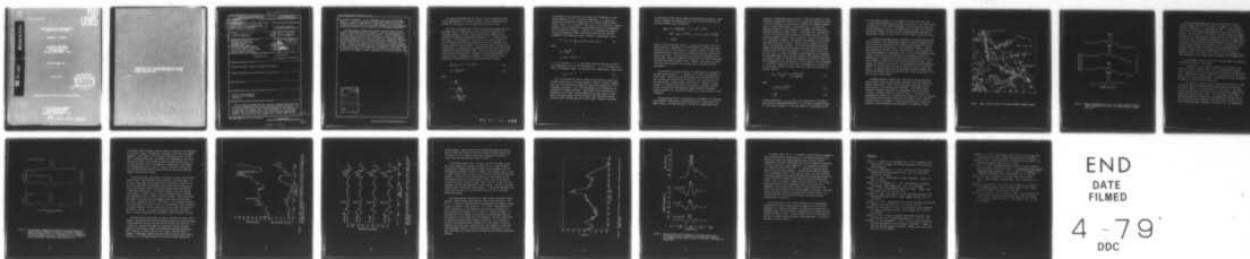
UNCLASSIFIED   SCIENTIFIC-1   AFGL-TR-78-0271   NL
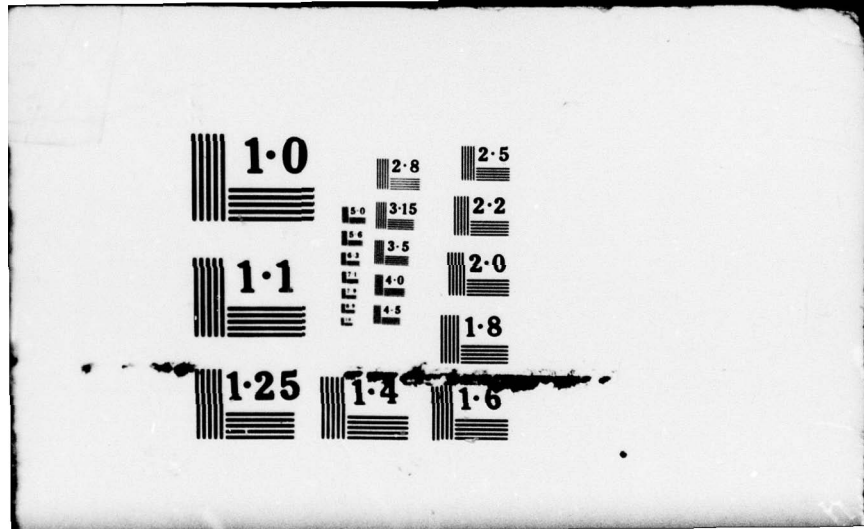
| OF |
ADA
064662

END
DATE
FILMED
4 -79
DDC

AFGL-TR-78-0271

LEV

INVESTIGATION OF THE LONG-WAVELENGTH
GRAVITY FIELD OF THE OCEANS

Micheline C. Roufosse

Smithsonian Institution
Astrophysical Observatory
60 Garden Street
Cambridge, Massachusetts 02138

Scientific Report No. 1

October 1978

FEB 15 1979

(14) SCIENTIFIC-1

(19) REPORT DOCUMENTATION PAGE		READ INSTRUCTIONS BEFORE COMPLETING FORM
(18) 1. REPORT NUMBER AFGL-TR-78-0271	2. GOVT ACCESSION NO.	3. RECIPIENT'S CATALOG NUMBER
(6) 4. TITLE (and Subtitle) INVESTIGATION OF THE LONG-WAVELENGTH GRAVITY FIELD OF THE OCEANS		5. TYPE OF REPORT & PERIOD COVERED Scientific Report No. 1
		6. PERFORMING ORG. REPORT NUMBER
(10) 7. AUTHOR(s) Micheline C. Roufosse		8. CONTRACT OR GRANT NUMBER(s) (15) F19628-78-C-0003 new
9. PERFORMING ORGANIZATION NAME AND ADDRESS Smithsonian Institution Astrophysical Observatory 60 Garden Street Cambridge, MA. 02138		10. PROGRAM ELEMENT, PROJECT, TASK AREA & WORK UNIT NUMBERS 61102F (16) 2309 (17) G1
11. CONTROLLING OFFICE NAME AND ADDRESS Air Force Geophysics Laboratory Hanscom AFB, Massachusetts 01731 Monitor/Thomas P. Rooney/LWG		(11) 12. REPORT DATE October 1978
		13. NUMBER OF PAGES 22
14. MONITORING AGENCY NAME & ADDRESS(if different from Controlling Office) (12) 24p.		15. SECURITY CLASS. (of this report) Unclassified
		15a. DECLASSIFICATION/DOWNGRADING SCHEDULE

16. DISTRIBUTION STATEMENT (of this Report)

Approved for public release; distribution unlimited.

17. DISTRIBUTION STATEMENT (of the abstract entered in Block 20, if different from Report)

18. SUPPLEMENTARY NOTES

19. KEY WORDS (Continue on reverse side if necessary and identify by block number)

Free air gravity anomalies
Flexure of the lithosphere
Convection

20. ABSTRACT (Continue on reverse side if necessary and identify by block number)

The correlation between the short wavelength features contained in the gravity and topographic height fields have been studied statistically. It is found that the slope of linear regression between the two fields varies with the age of the basement rocks. This observation is in qualitative agreement with the variations of P-wave velocity anomalies with tectonic classes. These results have been compared with a thermal model for the ——→(over)

DD FORM 1473 1 JAN 73 EDITION OF 1 NOV 65 IS OBSOLETE

044 850

continental lithosphere. As the lithosphere moves away from the ridge where it is created it thickens and induces the topography to sink down. Assuming a depth of compensation of at most 400 km, it is possible to calculate the evolution of the relationship between gravity and topographic height as a function of age and compare it with the observed quantities.

The geoid heights derived from the GEOS-3 altimeter data are also studied. Two methods are being developed in order to interpret the whole range of signals contained in the geoid heights. They each address a different class of events and thus complement each other in their ability to provide information on the state of convection in the earth's mantle. The long wavelength section of the spectrum yields information on the depth of the convection cells and the viscosity variations inside those cells through a study of the variations of the admittance as a function of wavelength. The short wavelength section of the spectrum provides information on the time evolution of the lithosphere, considered as a thin elastic plate, by studying its response to loads at several points in its evolution. The variation of the flexural rigidity with age will be obtained from that study.

ACCESSION for

NTIS	White Section	
DDC	Buff Section	☐
UNANNOUNCED		☐
JUSTIFICATION		

BY
DISTRIBUTION/AVAILABILITY CODES

Dist.	AVAIL. and/or SPECIAL
A	

The research performed under this grant is to gain information on the lateral heterogeneities in the earth's mantle. Several methods have been employed for that purpose; they are described in the next section.

The first investigation was a study of the correlation between the short-wavelength features in the gravity field of the earth and those of the topographic heights. For this, linear regression lines between free-air anomalies and topographic heights were obtained in $5° \times 5°$ squares for the whole world. The distribution of the slopes of the regression lines was then investigated statistically according to the age of the basement rocks for the continental regions studied. The slopes were found to increase with increasing age. That observation was compared with models for the continental lithosphere (Crough and Thompson, 1976), in which the heat-flow equation was solved to derive expressions for lithospheric thickening and subsidence as a function of age. Lithospheric thickening L' and subsidence S' can be expressed as a function of age t in dimensionless form as follows:

$$\frac{5}{3} [-\ln (1 - L') - L'] - \frac{L'^2}{3} = t' \quad , \tag{1}$$

$$S' = \frac{L'(3 + L')}{8} \quad , \tag{2}$$

where

$$L' = \frac{LQ}{kT_m} \quad ,$$

$$t' = t \frac{4Q^2}{k_\rho C_\rho T_m^2} \quad ,$$

$$S' = S \frac{Q(\rho_0 - \rho_w)}{kT_m^2 \rho_0 \alpha}$$

1

In the above, Q is the heat flux at the base of the lithosphere; k is the thermal conductivity; T_m is the melting temperature; ρ, ρ_0, and ρ_w are, respectively, the density at temperature T, the density at 300°K, and the density of water; C_p is the specific heat; and α is the coefficient of thermal expansion. We thus obtained the long-wavelength behavior of the topography and the lithospheric thickness. Similarly, using techniques discussed by Sclater and Francheteau (1970), we obtained an expression for the time dependence of the temperature, which is written in dimensionless form as

$$T' = (1 - z') + \sum_n a_n \sin (n\pi z') \exp - (\beta_n x') \quad , \tag{3}$$

where

$$a_n = \frac{2(-1)^{n+1}}{n\pi} \quad ,$$

$$\beta_n = (R^2 + \pi^2 n^2)^{1/2} - R \quad ,$$

$z = Lz'$ is the depth, $x = Lx'$ is the distance from the ridge axis (and therefore proportional to the age and plate velocity), $T = T_m T'$ is the temperature, and R is the Reynolds number. We then derived the lateral density changes using

$$\rho = \rho_0 (1 - \alpha \Lambda T) \quad . \tag{4}$$

Next, we evaluated the free-air anomalies associated with columns that are 400 km deep (which is the depth proposed in order for isostatic compensation to be fully achieved) and composed of appropriate proportions of crust, lithosphere, and mantle. For a first approximation, full integration over the whole plate seemed unnecessary. When Lambeck (1972) performed such an integration in his study of gravity anomalies over ocean ridges, he found that at a distance greater than 200 km from a ridge, the gravity anomaly associated with it had decreased to insignificance. Therefore, we decided

2

to calculate only those gravity anomalies associated with cylindrical columns 100 km in diameter and separated from each other by more than 500 km. We used the following simple relationship:

$$g_{400} = 2\pi G \times 10^8 \left(\rho_m \{ 400 - \ell + s'' + (50^2 + \ell^2)^{1/2} - [50^2 + (400 + s'')^2]^{1/2} \} + \rho_\ell \left[\ell + 50 - (50^2 + \ell^2)^{1/2} \right] \right)$$

$$- 308.6s'' \quad , \tag{5}$$

where G is the gravitational constant, ρ_m and ρ_ℓ are the mantle and lithospheric densities, respectively ℓ is the lithospheric thickness expressed in kilometers, and s'' is the elevation in kilometers; equation (5) works only when the continental regions that have undergone the largest subsidence are taken as the origin. The predictions are in qualitative agreement with observed slopes. We further compared the predictions with seismic observations using data published by Sengupta (1975). Sengupta's work shows an increase in P-wave velocity anomalies with increasing age, in agreement with our observations.

In the course of the above research, we became aware of shortcomings in the data used, which were 1° × 1° averages of the gravity and topographic-height fields. Specifically, the gravity data had large uncertainties and poor coverage over large portions of the oceans, which constitute one of the easiest places to begin studying time evolution. Therefore, we used raw data, on a track-by-track basis, from the Geos 3 altimeter, available at SAO. Utilizing the short-wavelength signals contained in the geoid heights analyzed so far, we obtained information on the time behavior of the lithosphere.

Following Crough (1975), we can consider the lithosphere as a thin plate whose thickness increases with increasing time up to a certain age, of the order of 80 m.y., and then continues to increase at a progressively lower

3

rate until it reaches equilibrium thickness. Since the thickness of a plate influences its mechanical properties, it is possible to study the time evolution of the lithosphere by observing how it deforms when loaded by seamounts placed at several points along its evolutionary path. To examine the mechanical properties of the lithosphere, we assumed the thin-plate model developed by McKenzie and Bowin (1976). In this model, the lithosphere consists of a thin elastic plate overlying a fluid medium; the plate is being loaded by bathymetric features such as seamounts, island chains, and ridges and is subsequently deformed. The magnitude and wavelength of the deformed area depend mostly on the flexural rigidity, which is proportional to the cube of the lithospheric thickness. By studying the correlation function between the geoid height and the bathymetry, we can determine the flexural rigidity of the area under investigation. This can be done in one of two ways: the first is to Fourier-transform the geoid height and the bathymetry into wavenumber space, divide the geoid height by the bathymetry, and obtain the response function as a function of wavelength; the flexural rigidity can then be deduced from the characteristics of this function. The second method is to calculate a theoretical filter $Z(k)$ in wavenumber space by using the thin-plate model (McKenzie and Bowin, 1976) and varying the values for the flexural rigidity:

$$Z(k) = \frac{3(\rho_c - \rho_w)}{2r\rho_e\gamma} \frac{(1 - e^{-wkt}) e^{-wkd}}{[1 + (wk)^4] wk} \tag{6}$$

where

$$\gamma = \left[\frac{(\rho_m - \rho_c) g}{F} \right]^{1/4}, \tag{7}$$

$$w = \frac{2\pi}{n\Delta\gamma} . \tag{8}$$

In these expressions, ρ_c, ρ_w, ρ_m, and ρ_e, are, respectively, the crustal, water, mantle, and mean-earth densities, r is the earth's equatorial radius, t is the crustal thickness, d is the water depth, g is the average gravity,

4

F is the flexural rigidity, n is the number of points in the filter, and Δ is the spacing between consecutive points of the filter. The filter derived in equation (6) is then Fourier-transformed into direct space and convolved with the bathymetry, resulting in a theoretical geoid height. The value for the flexural rigidity that gives the best agreement between predicted and observed geoid heights is the one that will be selected for each area studied.

In practice, the method chosen will depend on the type of data available. The first method is more adequate when comparing gravity and bathymetry data from surface ships because both sets of data give equispaced points and can thus be easily Fourier-transformed. The second method, however, is preferable when dealing with Geos 3 altimeter data because it is not dependent on having both bathymetry and geoid-height data in a Fourier-transformable format. The Geos 3 data are easily transformed, but the bathymetry data must be reconstructed, as rigorously as possible, along the subsatellite position by using bathymetric contour charts; this operation generally results in poor accuracy and irregular point spacing. The second method, the two-dimensional approach, is thus the one we have used to study the evolution of the lithosphere. The regions studied so far are the Hawaiian-Emperor Seamount chain, the Marshall-Gilbert Island chain, and the Crozet Islands, these areas will be part of a much larger network.

The Hawaiian-Emperor Seamounts were selected first because they have been previously studied by other methods from other sets of data (Watts and Cochran, 1974; Walcott, 1976). This area therefore constitutes an ideal testing ground for the two-dimensional technique. The altimeter passes from Geos 3 selected in that area are superposed on a map of the region in Figure 1, and their profiles are shown in Figure 2. The profiles are represented with respect to a reference geoid of degree and order 12 calculated from Standard Earth IV spherical-harmonics coefficients; they all show the features typical of the region — a sharp peak centered on the island chain flanked by a shallow depression and superposed on an asymmetrical bulge.
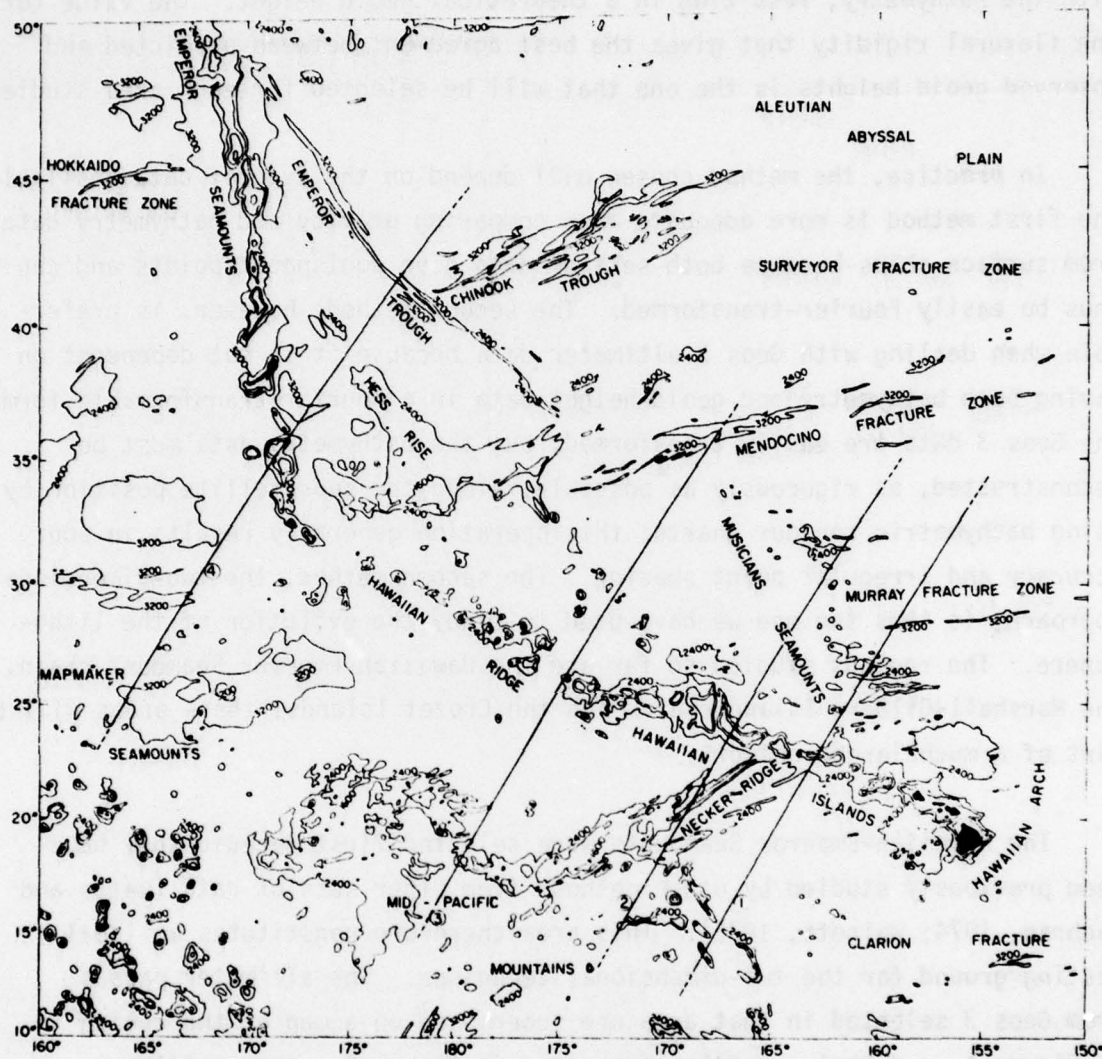
5

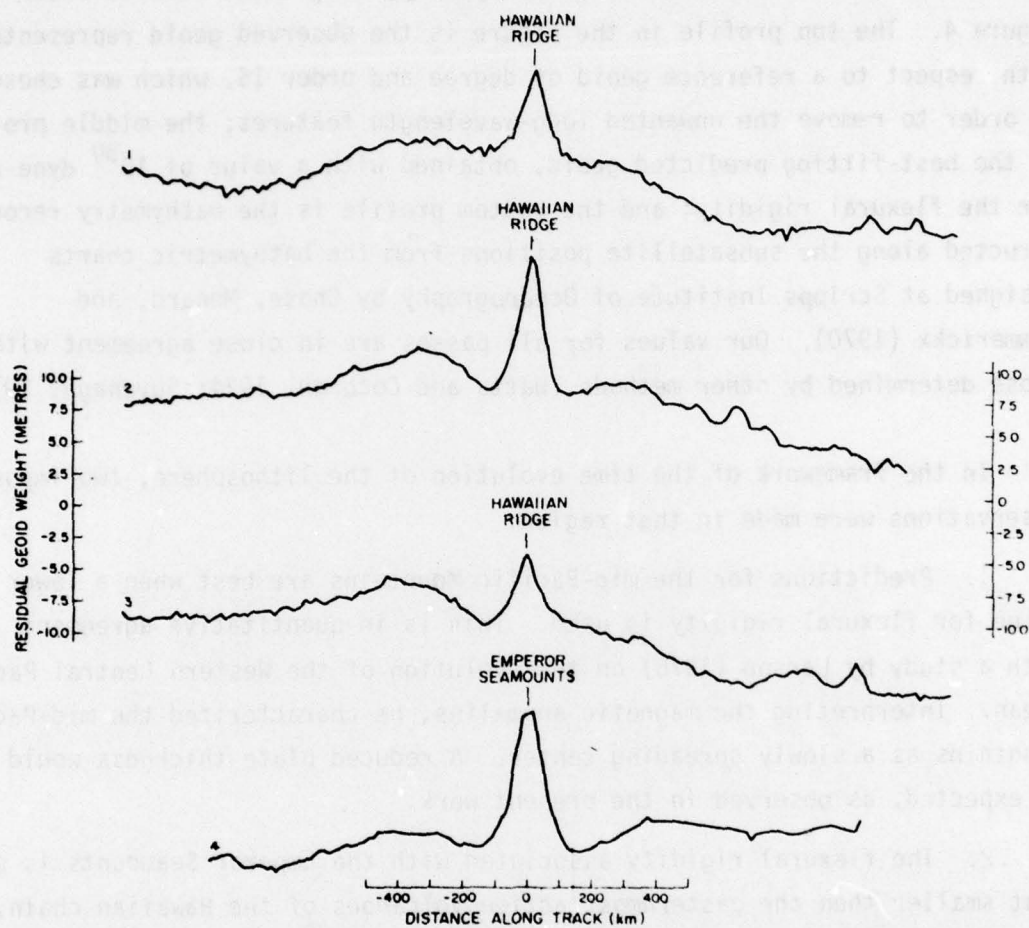Figure 1. Geos 3 passes studied in the Hawaiian-Emperor Seamount region.

Figure 2. Observed geoid-height profiles in the Hawaiian-Emperor Seamount region, represented with respect to a reference geoid of degree and order 12.

We then calculated theoretical filters using values for flexural rigidity ranging from 10^{29} to 10^{31} dyne-cm; an example, with a flexural rigidity of 10^{30} dyne-cm, is represented in Figure 3. After convolving the filters with the reconstructed bathymetry, we got the results shown in Figure 4. The top profile in the figure is the observed geoid represented with respect to a reference geoid of degree and order 16, which was chosen in order to remove the unwanted long-wavelength features; the middle profile is the best-fitting predicted geoid, obtained with a value of 10^{30} dyne-cm for the flexural rigidity; and the bottom profile is the bathymetry reconstructed along the subsatellite positions from the bathymetric charts designed at Scripps Institute of Oceanography by Chase, Menard, and Mammerickx (1970). Our values for all passes are in close agreement with those determined by other methods (Watts and Cochran, 1974; Suyenaga, 1977).

In the framework of the time evolution of the lithosphere, two important observations were made in that region:

1. Predictions for the mid-Pacific Mountains are best when a lower value for flexural rigidity is used. This is in quantitative agreement with a study by Larson (1976) on the evolution of the Western Central Pacific Ocean. Interpreting the magnetic anomalies, he characterized the mid-Pacific Mountains as a slowly spreading center. A reduced plate thickness would thus be expected, as observed in the present work.

2. The flexural rigidity associated with the Emperor Seamounts is somewhat smaller then the easternmost active volcanoes of the Hawaiian chain, as shown on Figure 5; it is on the order of 8×10^{29} dyne-cm. The smaller value can be explained by taking into account the age of the seamounts along the chain (Clague and Jarrard, 1973). In a recent study, Watts (1978) observed the correlation between gravity and bathymetry data obtained from surface ships over several sections of the Pacific Ocean: the East Pacific Rise, the Hawaiian-Emperor Seamounts, and the Kuril Rise. He deduced that
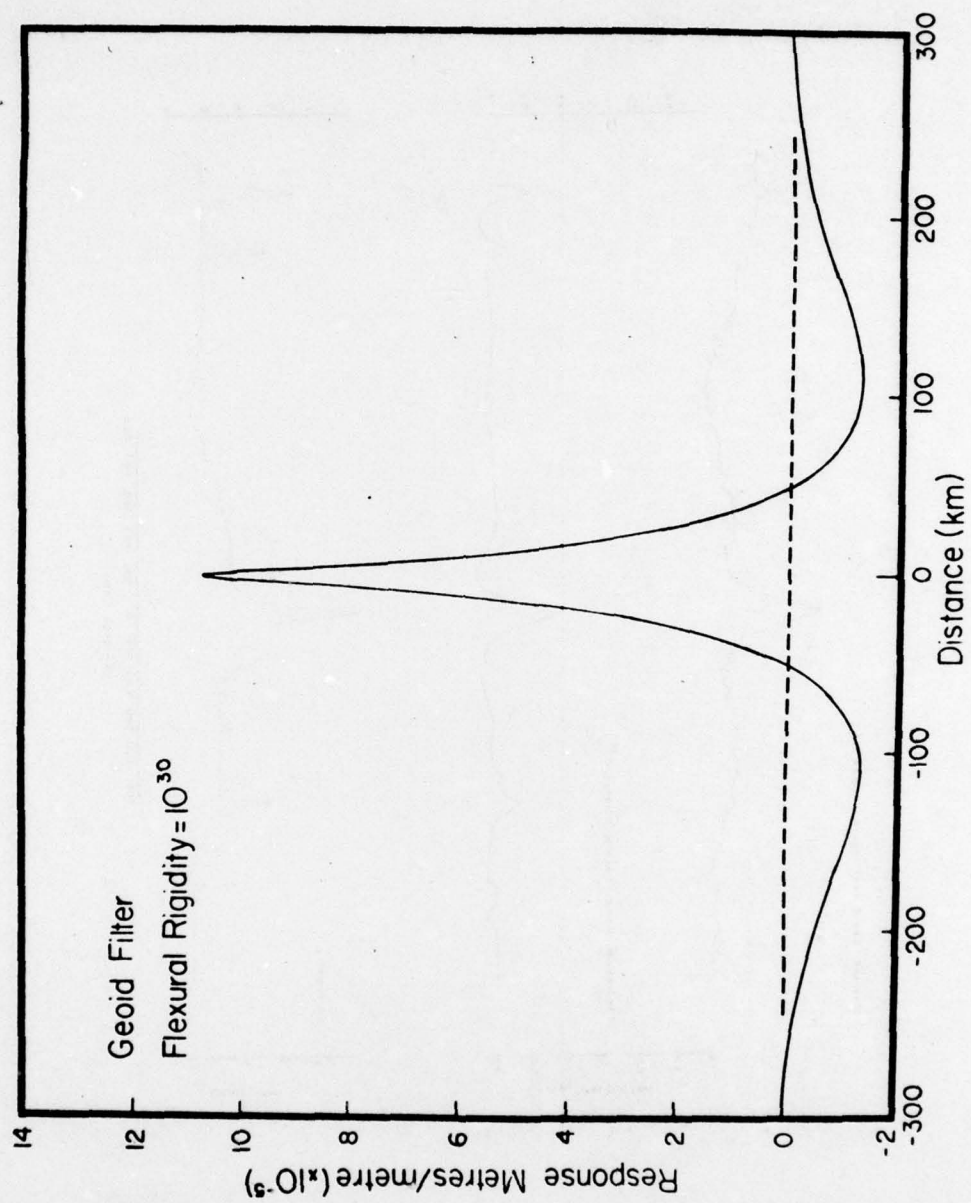
8

Figure 3. Theoretical geoid filter calculated with a flexural rigidity of 10^{30} dyne-cm.
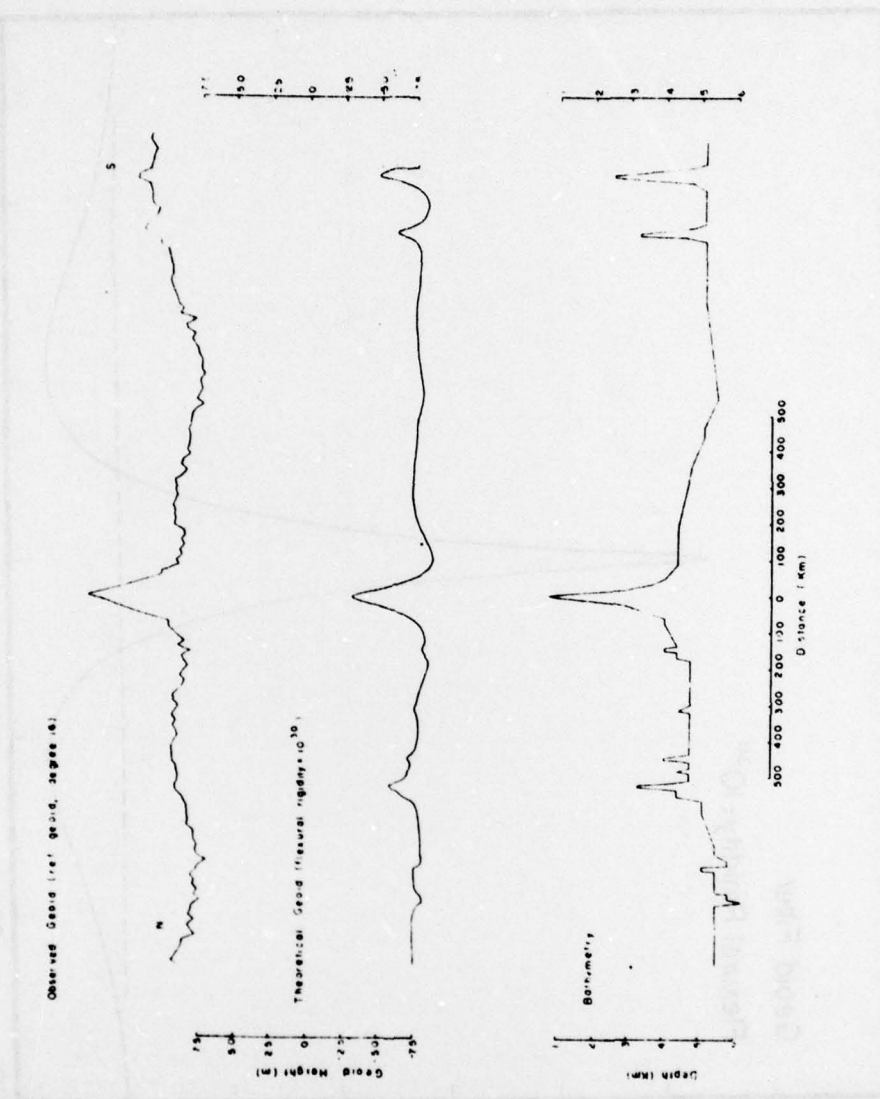
Figure 4. The top profile represents the observed geoid height with respect to a reference geoid of degree and order 16 in the Hawaiian region; the middle one is the predicted geoid, calculated with a filter of flexural rigidity of 10^{30} dyne-cm; it is con-volved with the bathymetry represented on the bottom profile.

10

Observed Geoid (ref geoid,degree 12)

Geoid Height (m)

N   S

Theoretical Geoid (flexural rigidity = 8×10²⁰)

Bathymetry

Depth (Km)

500 400 300 200 100 0 100 200 300 400 500
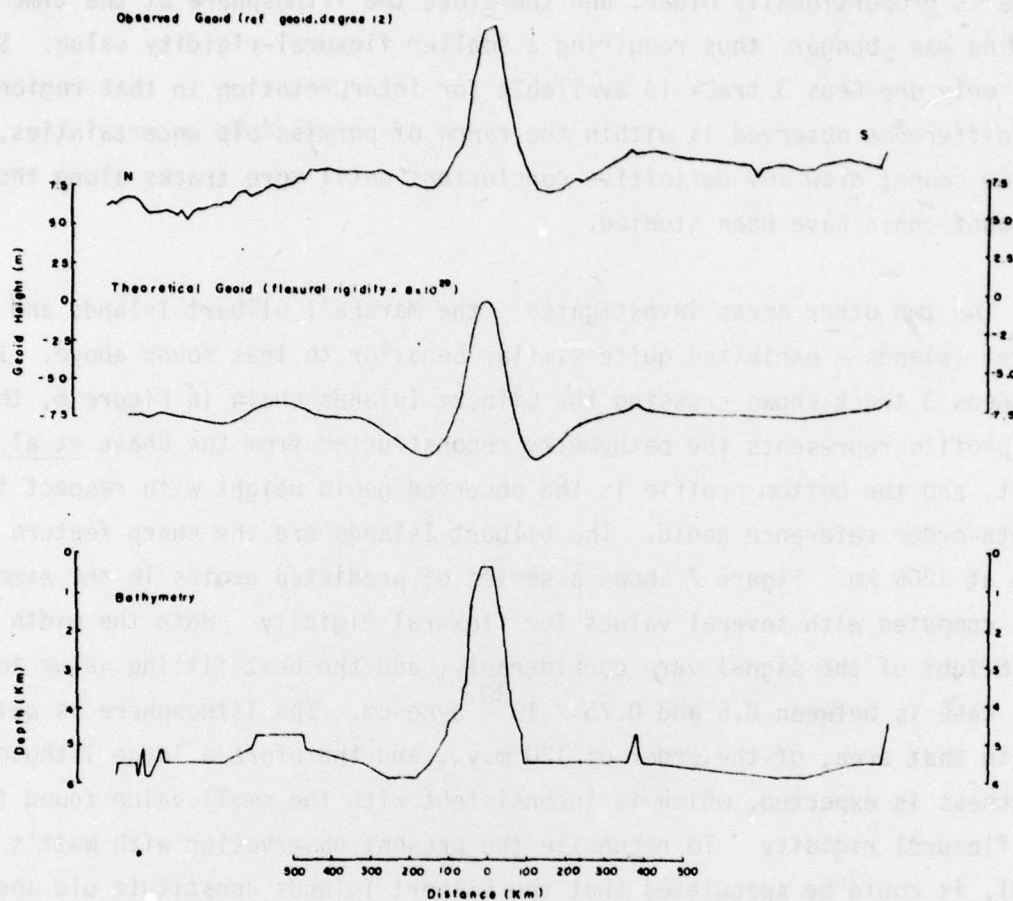Distance (Km)

Figure 5. The top profile represents the observed geoid with respect to a reference geoid of degree and order 12 in the Emperor Seamount region; the middle profile is the predicted geoid, calculated with a filter of flexural rigidity 8 × 10²⁹ dyne-cm; it is convolved with the bathymetry represented on the bottom profile.

11

the relevant factor related to flexural rigidity is the age of the lithosphere
at the time of loading. Although the lithosphere in the case of the Emperor
Seamounts is older than it is at the head of the Hawaiian chain, the load
there is proportionally older, and therefore the lithosphere at the time of
loading was younger, thus requiring a smaller flexural-rigidity value. So
far, only one Geos 3 track is available for interpretation in that region;
the difference observed is within the range of permissible uncertainties,
but we cannot draw any definitive conclusions until more tracks along the
seamount chain have been studied.

The two other areas investigated — the Marshall Gilbert Islands and the
Crozet Islands — exhibited quite similar behavior to that found above. In
the Geos 3 track shown crossing the Gilbert Islands chain in Figure 6, the
top profile represents the bathymetry reconstructed from the Chase et al.
chart, and the bottom profile is the observed geoid height with respect to
a 16th-order reference geoid. The Gilbert Islands are the sharp feature
seen at 1200 km. Figure 7 shows a series of predicted geoids in the same
area computed with several values for flexural rigidity. Both the width and
the height of the signal vary considerably, and the best-fitting value in
this case is between 0.5 and 0.75×10^{30} dyne-cm. The lithosphere is quite
old in that area, of the order of 120 m.y., and therefore a large lithospheric
thickness is expected, which is inconsistent with the small value found for
the flexural rigidity. To reconcile the present observation with Watt's
model, it could be speculated that the Gilbert Islands constitute old loads.

The study of the Crozet Plateau was done in collaboration with Dr. Anny
Cazenave, from Groupe de Recherche et de Géodesie Spatiale and Centre National
d'Etudes Spatiales, Toulouse, who provided the relevant Geos 3 profiles. In
a recent work, Cazenave and Lambeck (in preparation) analyzed the geoid
anomalies in that region using the three-dimensional approach developed by
Watts, Cochran, and Selzer (1975) for their study of the Great Meteor
Seamount. Cazenave and Lambeck found that flexural-rigidity values ranging
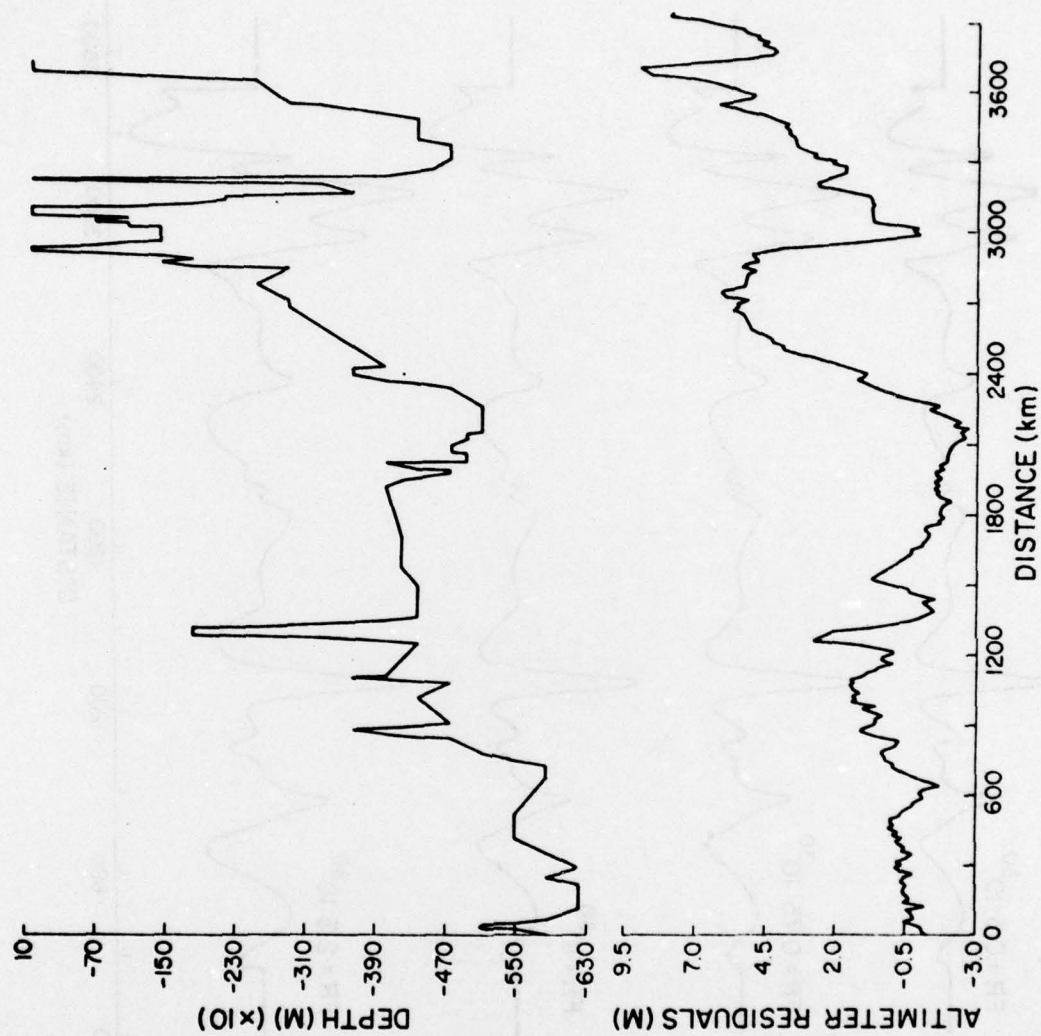from 0.75 to 1×10^{30} dyne-cm gave an excellent fit between observed and

Figure 6. The top profile represents the bathymetry in the Gilbert Islands region; the bottom profile represents the observed geoid with respect to a reference geoid of degree and order 16.
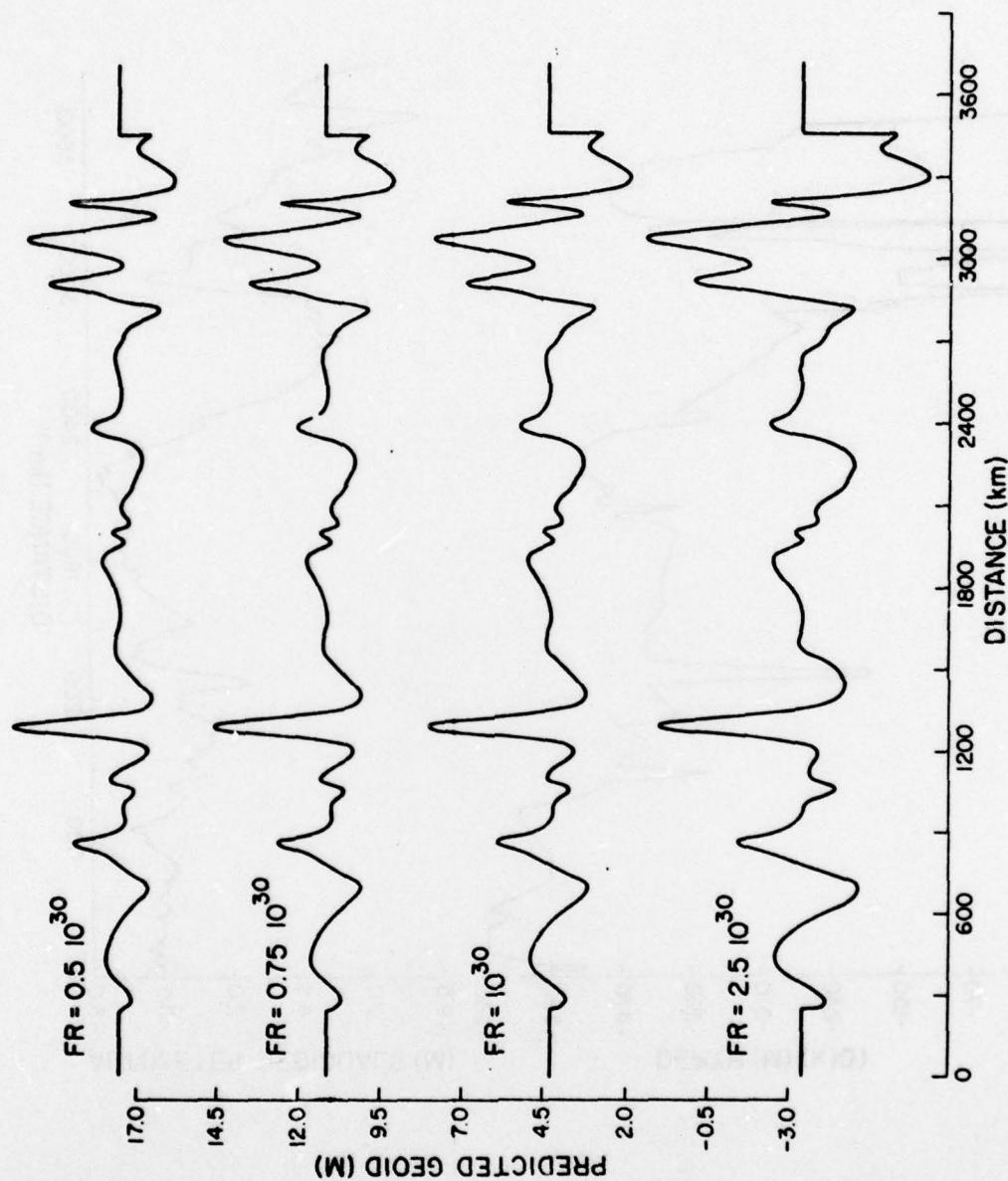
13

Figure 7. Four profiles of the predicted geoid in the Gilbert Islands region calculated with flexural-rigidity filters of 0.5, 0.75, 1, and 2.5 ($\times 10^{30}$) dyne-cm, respectively.

14

predicted geoids. When we applied the two-dimensional approach described above to the Crozet Islands, we obtained a flexural-rigidity value similar to theirs; this can be seen by comparing the observed geoid plotted in Figure 8 and the predicted geoids shown in Figure 9.

In the Crozet Plateau region, the age of the load is unknown, and the age of the lithosphere, according to Schlich (1975), is Upper Cretaceous. A comparison of Cazenave and Lambeck's method with ours suggests that the two-dimensional approach is ideal for studying linear features such as island or seamount chains, while it offers less precision for dealing with individual features. In the case of the Crozet Plateau, only those tracks crossing the maximum altitude of the plateau gave a correct value for the flexural rigidity; all others resulted in larger values, owing to the fact that they reproduced only the lower bathymetric points, whereas, in reality, the actual observed geoid is influenced by nearby masses. In the future, therefore, the feature being studied will dictate whether we use the two- or the three-dimensional approach.

The long-wavelength interpretation of geoid heights offers more complex problems. Several attempts were made that did not prove successful. First, the $1° \times 1°$ averages of the geoid height and bathymetry were compared directly by using a program of linear regression. The results of that operation are totally inconclusive, as the comparison involves features belonging to a whole spectrum of wavelengths, each of which has a different response. To overcome part of that problem, we subtracted the long-wavelength features, which generally do not compare well with bathymetry, from the altimetry data by removing a reference geoid of degree and order 12. As we had found in our work in the Hawaiian-Emperor Seamount chain, this method is effective. Comparing the residual geoid heights and the total bathymetry, we obtained short-wavelength features in the geoid height with a magnitude of 10 m at most; they appear to be associated for the most part with distinct bathymetric features.
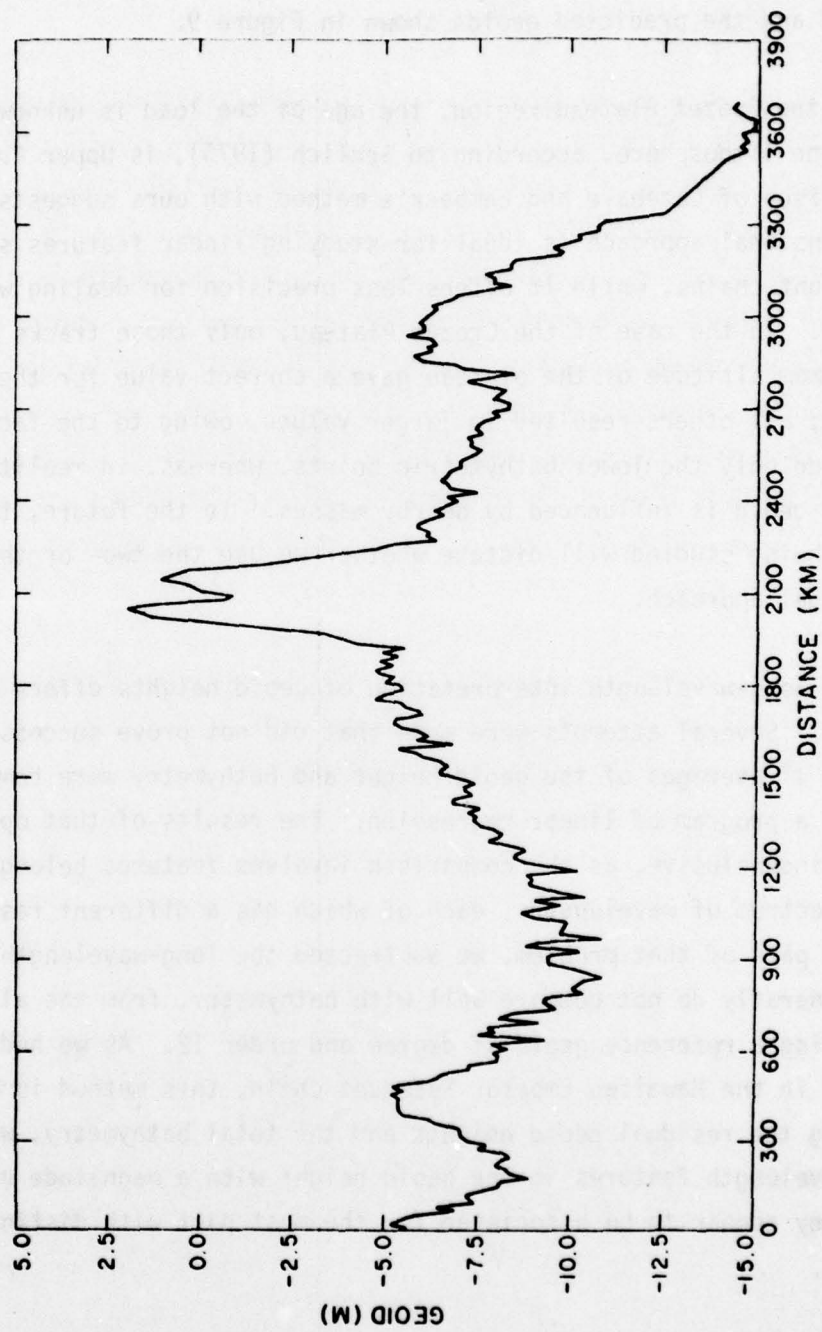
15

Figure 8. Observed geoid with respect to a reference geoid of degree and order 16 in the Crozet region.
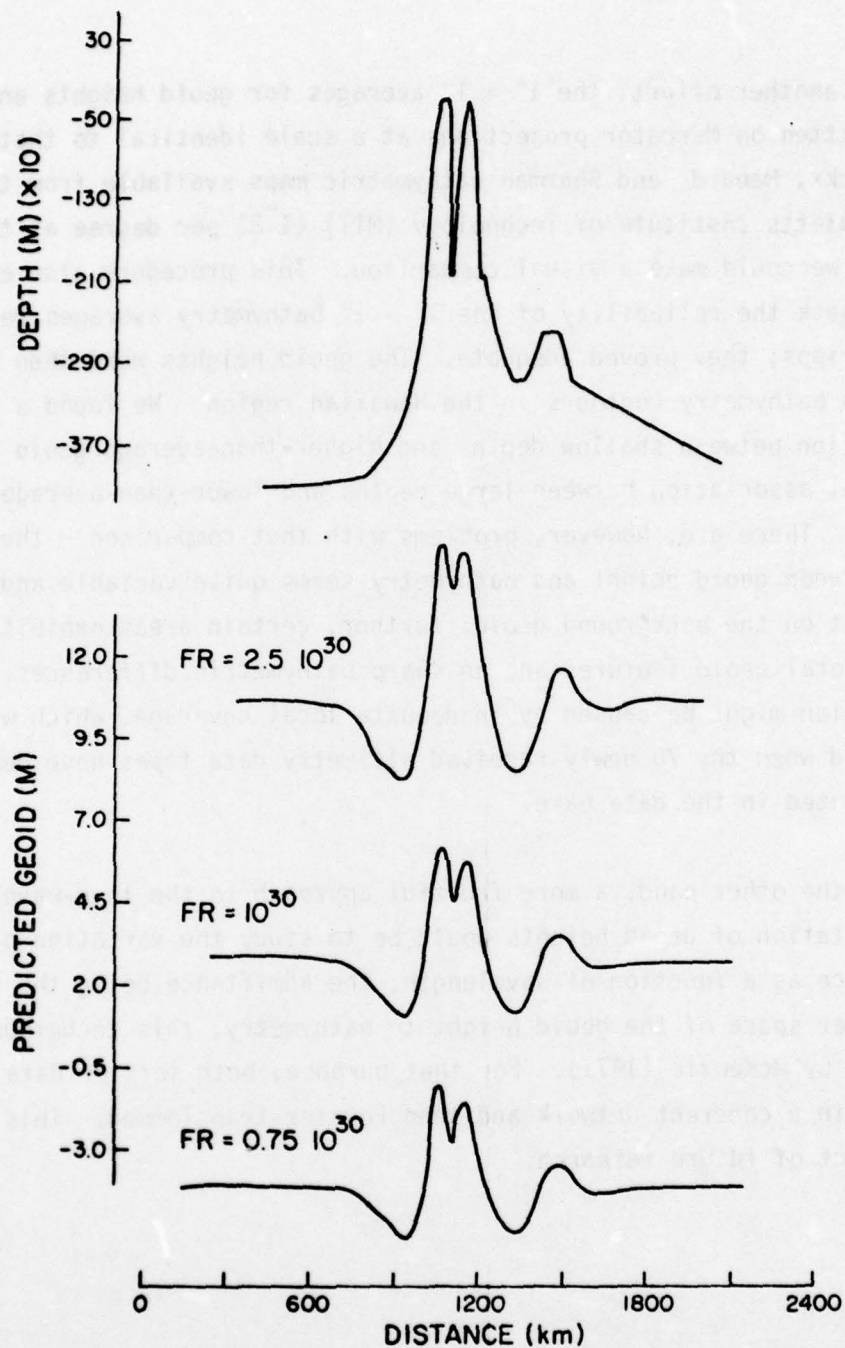
Figure 9. The top profile is the bathymetry in the Crozet region; the
three bottom profiles represent the predicted geoid calculated
with flexural-rigidity filters of 2.5, 1, and 0.75 ($\times 10^{30}$) dyne-cm,
respectively.

In another effort, the 1° × 1° averages for geoid heights and bathymetry were written on Mercator projections at a scale identical to that on the Mammerickx, Menard, and Sharman bathymetric maps available from the Massachusetts Institute of Technology (MIT) (1".21 per degree at the equator) so that we could make a visual comparison. This procedure also enabled us to check the reliability of the 1° × 1° bathymetry averages received from Scripps; they proved adequate. The geoid heights were then compared with the bathymetry contours in the Hawaiian region. We found a definite correlation between shallow depths and higher-than-average geoid heights and a general association between large depths and lower-than-average geoid heights. There are, however, problems with that comparison – the relationship between geoid height and bathymetry seems quite variable and is dependent on the background geoid; further, certain areas exhibit very marked local geoid features and no sharp bathymetric differences. The latter observation might be caused by inadequate local coverage, which will be rectified when the 70 newly received altimetry data tapes have been incorporated in the data base.

On the other hand, a more fruitful approach to the long-wavelength interpretation of geoid heights would be to study the variation of the admittance as a function of wavelength, the admittance being the ratio in wavenumber space of the geoid height to bathymetry; this technique has been proposed by McKenzie (1977). For that purpose, both sets of data must be written in a coherent network and then Fourier-transformed. This will be the object of future research.

18

References

Chase, T. E., Menard, H. W., and Mammerickx, J., 1970. Bathymetry of the North Pacific. Scripps Institution of Oceanography and Institute of Marine Resources.

Clague, D. A., and Jarrard, R. D., 1973. Tertiary Pacific Plate motion deduced from the Hawaiian-Emperor chain. Geol. Soc. Amer. Bull., vol. 84, pp. 1135-1154.

Crough, S. T., 1975. Thermal model of oceanic lithosphere. Nature, vol. 256, pp. 388-390.

Crough, S. T., and Thompson, G. A., 1976. Thermal model of continental lithosphere. Journ. Geophys. Res., vol. 81, pp. 4857-4862.

Lambeck, K., 1972. Gravity anomalies over ocean ridges. Geophys. Journ. Roy. Astron. Soc., vol. 30, pp. 37-53.

Larson, R. L., 1976. Late Jurassic and early Cretaceous evolution of the Western Central Pacific Ocean. Journ. Geomagn. Geochem., vol. 28, pp. 219-236.

McKenzie, D. P., 1977. Surface deformation, gravity anomalies and convection. Geophys. Journ. Roy. Astron. Soc., vol. 48, pp. 211-238.

McKenzie, D. P., and Bowin, C., 1976. The relationship between bathymetry and gravity in the Atlantic Ocean. Journ. Geophys. Res., vol. 81, pp. 1903-1915.

Schlich, R., 1975. Structure et age de l'Océan Indien Occidental. Mém. Hors-Sene No. 6 de la Société Géologique de France, Paris, p. 103.

Sclater, J. G., and Francheteau, J., 1970. The implication of terrestrial heat flow observations on current tectonic and geochemical models of the crust and upper mantle of the earth. Geophys. Journ. Roy. Astron. Soc., vol. 20, pp. 509-542.

Sengupta, M. K., 1975. The structure of the earth's mantle from body wave observations. Ph.D Thesis, Massachusetts Institute of Technology.

Suyenaga, W., 1977. Earth deformation in response to surface loading. EOS, Trans. Amer. Geophys. Union, vol. 58, p. 1231.

Walcott, R. I., 1976. Lithospheric flexure, analysis of gravity anomalies and the propagation of seamount chains. In The Geophysics of the Pacific Ocean Basin and Its Margin, ed. by G. H. Sutton, M. H. Manghnani, and R. Moberly, AGU Geophys. Mono. 19, Washington, D.C., pp. 431-438.

Watts, A. B., 1978. An analysis of isostasy in the world's oceans: Part I — Hawaiian-Emperor Seamount chain. Journ. Geophys. Res. (in press).

Watts, A. B., and Cochran, J. R., 1974. Gravity anomalies and flexure of the lithosphere along the Hawaiian-Emperor Seamount chain. Geophys. Journ. Roy. Astron. Soc., vol. 38, pp. 119-141.

Watts, A. B., Cochran, J. R., and Selzer, G., 1975. Gravity anomalies and flexure of the lithosphere: A three-dimensional study of the Great Meteor Seamount, Northeast Atlantic. Journ. Geophys. Res., vol. 80, pp. 1391-1398.

20